

Hybrid Affine Registration Using Intensity Similarity and Feature Similarity for Pathology Detection

김준식 · 김호성 · 이종민 · 김재석 · 김인영 · 김선일

한양대학교 의공학교실

(2001년 7월 20일 접수, 2001년 12월 29일 채택)

Hybrid Affine Registration Using Intensity Similarity and Feature Similarity for Pathology Detection

June-Sic Kim, Ho-Sung Kim, Jong-Min Lee, Jae-Seok Kim, In-Young Kim, and Sun I. Kim

Dept. of Biomedical Engineering, Hanyang University

(Received July 20, 2001. Accepted December 29, 2001)

요약 : 본 연구의 목적은 선형 변환을 이용한 레지스트레이션의 정확도를 높이는 데 있다. 서로 다른 개인간의 뇌영상을 비교분석하기 위해서는 공통된 좌표계로 각 영상을 변환하는 작업이 필요하다. 정확한 변환을 위해서는 전체적인 뇌영상의 매치와 국소적 영역의 매치가 모두 중요하다. 일반적으로 상호정보를 이용한 레지스트레이션은 전체적인 뇌영상을 매치시키는데 유리하다. 그러나 관심영역에 대한 매치는 특징기반 레지스트레이션 방법이 더 유리하다. 본 논문에서 제시하는 통합 레지스트레이션은 특징정보와 더불어 복셀기반의 상호정보를 함께 사용하였다. 이러한 접근 방법은 정신분열증을 판단하는 기준으로 많이 사용되는 뇌량을 포함하는 뇌의 중심부분의 매칭에 유리함을 실험을 통해 확인하였다. 상호정보만을 사용하는 복셀기반 레지스트레이션이나 탈라이락 좌표계를 이용한 정규화에 비해 본 연구의 통합 레지스트레이션은 전체적 뇌영상 뿐만 아니라 관심영역에서의 레지스트레이션 오차가 더 작았다.

Abstract : The objective of this study is to provide a precise form of spatial normalization with affine transformation. The quantitative comparison of the brain architecture across different subjects requires a common coordinate system. For the common coordinate system, not only global brain but also a local region of interest should be spatially normalized. Registration using mutual information generally matches the whole brain well. However, a region of interest may not be normalized compared to the feature-based methods with the landmarks. The hybrid method of this paper utilizes feature information of the local region as well as intensity similarity. Central gray nuclei of a brain including corpus callosum, which is used for feature in Schizophrenia detection, is appropriately normalized by the hybrid method. In the results section, our method is compared with mutual information only method and Talairach mapping with schizophrenia patients, and is shown how it accurately normalizes feature.

Key words : Mutual information, Feature similarity, Spatial normalization

INTRODUCTION

Image registration was an important component in many neuroimaging applications using multi-modality and intra-modality medical images. The geometric alignment of multi-modality images was a fundamental task in

numerous applications in three-dimensional (3D) medical image processing. Medical diagnosis, for instance, often benefited from the complementarity of the information in images of different modalities. In radiotherapy planning, dose calculation was based on the computed tomography (CT) data, while tumor outlining was often better performed in the corresponding magnetic resonance (MR) scan. For brain function analysis, MR images provided anatomical information while functional information might be obtained from positron emission tomography (PET)

images, etc. Moreover, the image registration allowed the characterization of the morphology of different subjects' brains. MR images which represented brain structure were generally used for the morphologic analysis and comparison. For the comparison, every brain images were normalized in the same stereotactic space. There were many methods for registration such as including Talairach mapping, linear transformation, and non-linear deformation. Studies of brain morphometry had already revealed structural differences between a number of patient populations, and much of the focus of brain disease research as schizophrenia in particular was based upon brain morphometry[1, 2, 3].

Image registration could be broadly divided into label based and non-label based. Label-based techniques identified homologous features in the image and template and found the transformations that best superposed them. The labels could be frame, points, lines, or surfaces[4, 5, 6,].

Stereotactic frame-based registration, one of the label-based methods, was very accurate. But this method was inconvenient, and difficult to apply retrospectively, as with any external point landmark-based method. If the labels were points, then the required transformation at each of those points was well known. However, anatomical point landmark methods were usually labor intensive and the accuracy depended on the accurate indication of corresponding landmarks in all modalities. Label-based registration required delineation of corresponding surfaces in each of the images separately. But surface segmentation algorithms were highly data and application dependent and surfaces were not easily identified in functional modalities such as PET.

Non-label based approaches identified a spatial transformation that minimized some index of the difference between an object and a target images, where both were treated as unlabeled continuous processes. The matching criterion was usually based upon maximizing the correlation between the images. For this criterion to be successful, it required an image itself. In other words, there should be correspondence in the gray levels of the different tissue types between the object and target. Various voxel-based methods had been proposed that optimized some global measure of the absolute difference between image intensities of corresponding voxel within overlapping parts or in a region of interest (ROI)[7, 8, 9, 10]. The advantage of voxel-based methods was that feature calculation was straightforward or even absent when only gray-values were used, so that the accuracy of these methods was

not limited by segmentation errors as in surface based methods. These criteria all relied on the assumption that the intensities of the two images were linearly correlated, which was generally not satisfied in the case of inter-modality registration. Advanced correlation measure using mutual information (MI) registered inter-modality image as well as intra-modality[11]. The MI registration criterion provided accurate, highly robust, and completely automatic registration of multi-modality and intra-modality medical images. However, these voxel-based approaches were difficult to match the complex structure of a brain because these methods used global intensity similarity only. Geometric information was absent in these methods.

In this paper, we provide a hybrid method with affine transformation using valuable characteristics of label based and non-label based by means of maximizing both of intensity similarity using MI criterion and feature similarity. This approach matches the global form of a brain through the intensity correlation, and also registers a local anatomic region with the homologous features. In our study, anterior commissure (AC) and posterior commissure (PC) is used as the feature. These points is important to chart the central gray nuclei and the mesencephalic region in the Talairach system[12]. In order to validate our algorithm, the registration error of the global brain and the corpus callosum will be estimated in the mutual information only method, the Talairach mapping and our method.

MATERIALS AND METHODS

An intensity-based brain template is used as a target image. In this study, registration algorithm requires intensity distribution of brain images and features such as AC and PC. The Talairach coordinate system satisfies this condition. The brain template is made with a normal case in the Talairach system (section 1). Then, suspected image data of disease are matched to the brain template with registration algorithm of section 2. Finally, each feature of the brain template and patient image is extracted and compared by method of section 3.

1. Intensity-based brain template for Koreans

10 normal brain images were used to make an averaged brain atlas. To preserve the morphological characteristic of the middle part of the brain including the corpus callosum and ventricles, the Talairach coordinate system was used. The Talairach coordinate system is the 3D stereotactic space based on AC and PC, mid-sagittal

plane, and 6 outer boundary planes of the brain. The intensity averaged brain atlas is generated as follows. Three-dimensional image data of all subjects are mapped into standardized Talairach space to correct differences in relative position and size. The intensity of each image is normalized. Then, the images are averaged on a voxel-by-voxel basis, producing an average intensity MRI dataset as shown in Figure 1.

2. Registration algorithm

Each of the volume data is associated with a volume coordinate frame. Its origin is positioned in a corner of the image with the x axis along the row direction, the y axis along the column direction, and the z axis along the plane direction. One of the images is selected to be the floating volume, F , transformed into reference volume, R . In this study, we apply affine transformation to the transformation T_p . The affine transformation is a superposition of a 3D rotation, translation, scaling, and shearing. Then the registration parameter p is a twelve-component vector. Transformation of volume coordinates P_F to P_R from volume F to volume R is given by

$$P_R = M_R^{-1} \cdot M_{\text{affine}} \cdot M_F \cdot P_F, \quad (\text{Eq. 1})$$

$$\text{where. } M_{\text{affine}} = \begin{bmatrix} P_{11} & P_{12} & P_{13} & P_{14} \\ P_{21} & P_{22} & P_{23} & P_{24} \\ P_{31} & P_{32} & P_{33} & P_{34} \\ 0 & 0 & 0 & 1 \end{bmatrix}$$

M_F and M_R are matrices that map from the voxel coordinates of images F and G into their own Euclidian space.

M_F and M_R are 4×4 matrixes representing the voxel size and the translation to the volume center of image F and R , respectively in Euclidian space. Often, the volumes (F and R) will have anisotropic voxels. The dimensions of the voxels are also likely to differ between images. For simplicity, a Euclidian space is used, where measures of distances are expressed in millimeters. Rather than interpolating the images such that the voxels are cubic and have the same dimensions in all images, one can simply define affine transformation matrixes that map from voxel coordinates into this Euclidian space.

The registration algorithm optimizes M_{affine} parameters maximizing similarity between volumes. To optimize parameters, we utilize both the intensity similarity and

feature similarity.

2-1. Intensity similarity

For optimizing the affine parameters, the cost function uses two terms. The first term is similarity measure of mutual information. The intensity cost function is defined by MI between $T_p(F)$ and R .

$$C_{\text{Intensity}} = I(T_p(F), R), \quad (\text{Eq. 2})$$

In this paper, we deal with the Kullback-Leibler measure of mutual information, for which an essential element is the joint histogram of the floating and reference image. We expect the histogram of the transformed test image to depend slightly on the transformation parameters, and the histogram of the reference image to be constant, exactly. The most important dependence with respect to the geometric transformation parameters is to be found in their joint histogram.

Estimations for the marginal and joint image intensity distributions $P_{F,p}(f)$, $P_{R,p}(r)$, and $P_{FR,p}(f, r)$ are obtained by normalization of a joint histogram $h_p(f, r)$

$$\begin{aligned} P_{FR,p}(f, r) &= \frac{h_p(f, r)}{\sum_{f,r} h_p(f, r)} \\ P_{F,p}(f) &= \sum_r P_{FR,p}(f, r) \\ P_{R,p}(r) &= \sum_f P_{FR,p}(f, r) \end{aligned} \quad (\text{Eq. 3})$$

The MI registration criterion is evaluated by

$$I(T_p(F), R) = \sum_{f,r} P_{FR,p}(f, r) \log_2 \frac{P_{FR,p}(f, r)}{P_{F,p}(f) \cdot P_{R,p}(r)}, \quad (\text{Eq. 4})$$

where T_p : affine transformation,

F, R : floating source and reference target images,

f : intensity value on F image mapped into R space by affine transformation,

r : intensity value on R image,

$P_{F,p}(f)$: the probability when the f value exist on the F image,

$P_{R,p}(r)$: the probability when the r value exist on the R image,

$P_{FR,p}(f, r)$: the probability when the f and r value simultaneously appear on same points in R space.

2-2. Feature similarity

The second term of total cost function consists of feature similarity. AC and PC points are used as features in this work. Since the corpus callosum is laid between AC and PC points, the corpus callosum is registered well if each of the AC and PC points is accurately matched. The feature term of the cost function is given by

$$C_{Feature} = -\sqrt{[T_p(AC_f) - AC_r]^2 + [T_p(PC_f) - PC_r]^2} \quad (\text{Eq. 5})$$

$C_{Feature}$ represents negative distance between feature points of floating and reference volume.

2-3. Registration criterion

The total cost function for optimization is defined by both the intensity and feature cost functions as the following.

$$C_{Total} = C_{Intensity} + \lambda C_{Feature}, \quad (\text{Eq. 6})$$

where λ is a scaling factor.

Finally, the optimal registration parameter p^* is found from

$$p^* = \arg \max_p C_{Total} \quad (\text{Eq. 7})$$

The affine transformation parameters are iteratively optimized and refined by Powell's multidimensional direction set method and Brent's line minimization algorithm[13]. The direction matrix is initialized with unit vectors in each of the parameter directions. Then, the iteration to the updated direction is performed. λ is also updated with every iterations. λ trades off matching the global brain

and coming close to features. If the parameter λ is constant and enough big, AC and PC points of floating volume are nearly registered into AC and PC points of reference volume, but the intensity cost function may not reach global minima. If λ is constant and too small, the global appearance of brain is well registered, but the local region of interest such as the corpus callosum may not be normalized. Therefore, we determine the parameter λ to be adaptable. If AC and PC of floating volume are far from reference, λ becomes large so that the cost function keeps an appropriate initial condition and avoids a local minimum. If AC and PC points of floating volume are near to them of reference, λ becomes small so that the cost function prevents them from mismatching brain volumes because of feature constraints. Therefore, the current scaling parameter λ^n is updated by

$$\lambda^n = \frac{C_{feature}^n}{C_{feature}^1} \times \lambda^1 \quad (\text{Eq. 8})$$

where n is the iteration number.

λ^1 is initial value of 0.003 in this study. This equation indicates that the scaling parameter is in proportional to the current feature cost value.

3. Feature extraction for Schizophrenia detection

A parcellation tool, developed by the biomedical engineering department in Hanyang University, is used to extract the corpus callosum and gray-matter[14]. This tool provides preprocessing operations, such as cerebrum extraction, segmentation, and boundary detection of region of interest (ROI). Region growing and morphological operations such as dilation and erosion were used to extract the cerebrum of the brain. In order to select ROI for the corpus callosum, the cerebrum is first classified

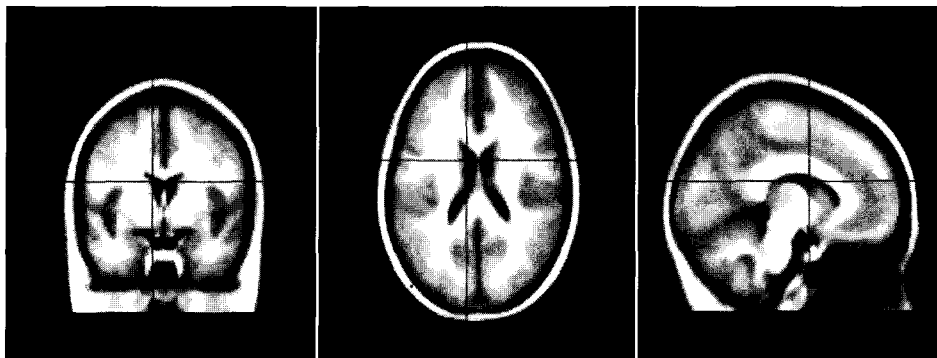


Fig. 1. Intensity-based Korean brain template

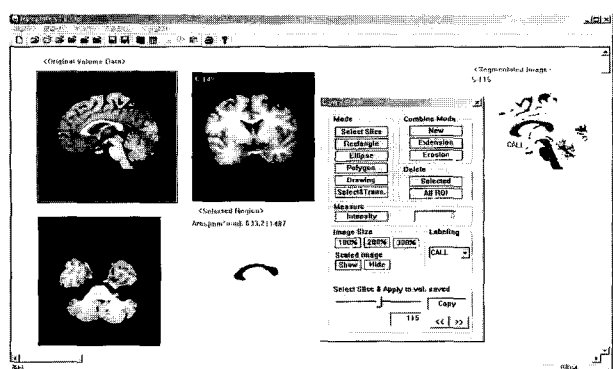


Fig. 2. ROI selection as feature

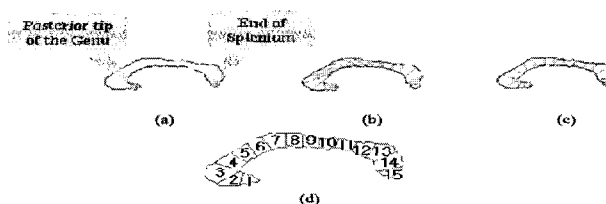


Fig. 3. Sectioning corpus callosum. (a) edge of corpus callosum, (b) initially sectioned corpus callosum, (c) finally sectioned corpus callosum, and (d) numbering section 1 to 15

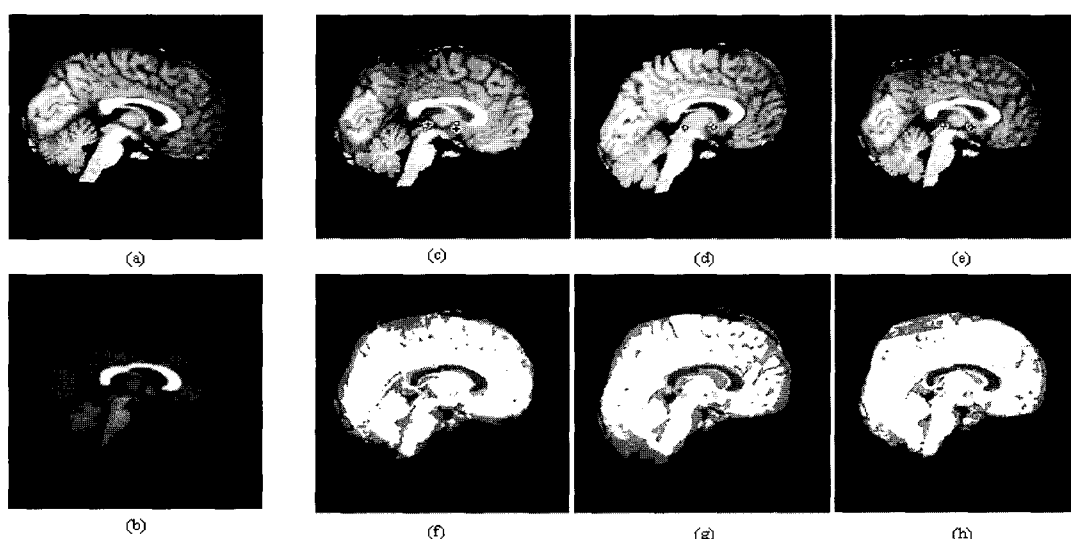


Fig. 4. The result image may be changeable with magnitude variation of the feature constraint parameter . (a) original source image which is not transformed (mid-sagittal plane), (b) target image (brain template, mid-sagittal plane), (c) small parameter $\lambda = 0.0001$ (AC and PC points were not well-matched between transformed points and targeting points), (d) large parameter $\lambda = 0.01$ (AC and PC points were well-matched however, the large constraint brought about geometric distortion), (e) adaptive parameter λ , (f)~(h) are the corresponding merged images between target image (brain atlas) and (c)~(e)

into several tissues—white matter (WM), gray matter (GM), and cerebrospinal fluid (CSF). The corpus callosum is included in WM. Since the selection of ROI is performed with the segmentation results, the accuracy of the analysis depends highly on the segmentation method. In order to improve segmentation results, fuzzy c-means (FCM) is repeatedly applied to data, which is classified as a WM class and whose resulting membership value is less than a threshold value[15]. The parcellation tool displays both the original image and its segmentation result. Then, the ROI is being drawn on the segmented image while simultaneously referenced to its original image. The ROI determined above is also displayed on the

original image for crosschecking. Figure 2 shows the corpus callosum extracted by the parcellation tool.

The edge of the cortex and the contour of the corpus callosum are traced by our parcellation tool (Figure 3(a)). Landmark points on the corpus callosum are located at the posterior tip of the genu and the end of the splenium. Next, 14 evenly spaced points on the spline curve are located between these points along the top and bottom edges of the corpus callosum as shown in Figure 3(b). Each of the 14 points on the top of the ROI is connected with its opposite member on the bottom. Center points of these connecting lines are calculated. Lines are drawn across the corpus callosum through these center points.

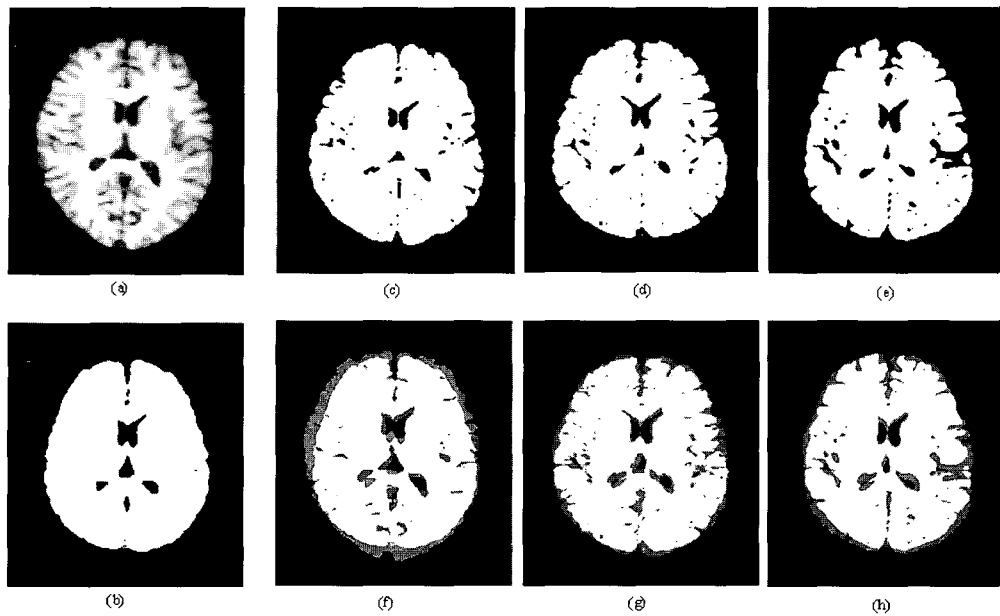


Fig. 5. shows result images of each method in axial plane. (a) original source image which is not transformed, (b) target image (brain template), (c) source image after hybrid registration, (d) source image after registration only using MI maximization, (e) source image after mapping into Talairach space, (c)~(e) images are binary image made by thresholding intensity, (f)~(h) are the corresponding merged images between target image (b) and each of (c)~(e)

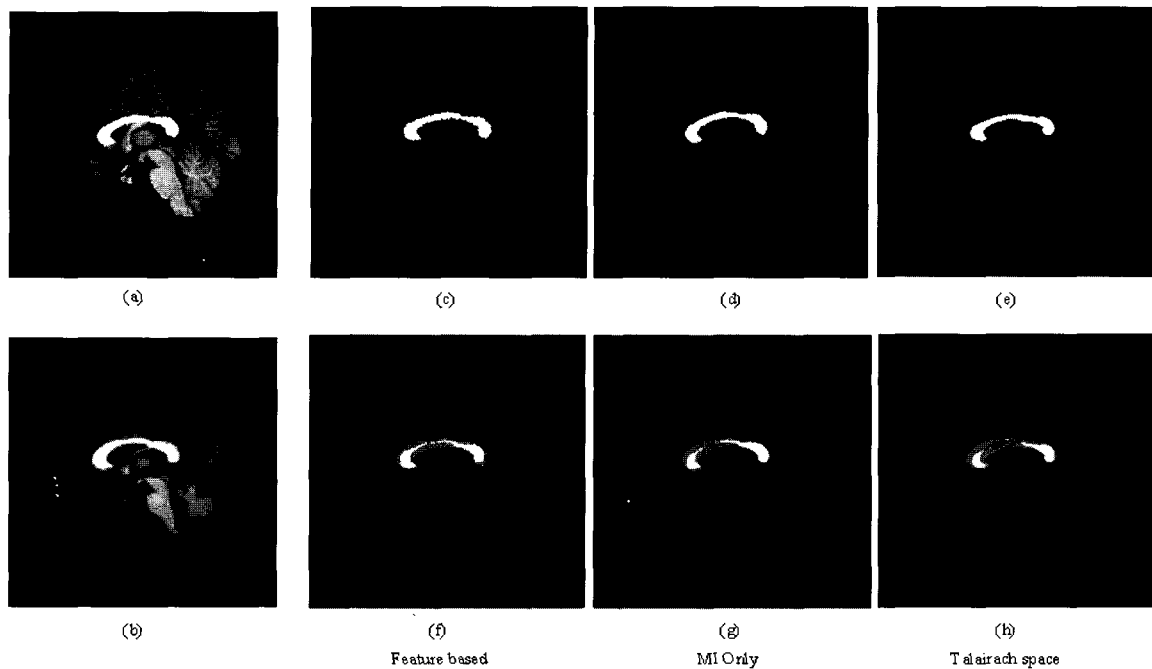


Fig. 6. The result images of each method are shown in mid-sagittal plane. (a) The source image before registration, (b) The target image (brain template), (c) corpus callosum extracted from source image after hybrid registration, (d) corpus callosum extracted from source image after registration only using MI maximization, (e) corpus callosum extracted from source image after mapping into Talairach space, (f)~(h) are the corresponding merged images between target image (brain atlas) and (c)~(e). The gray value of (f)~(h) means difference between atlas and each image (c)~(e)

Then, we redefine 14 sectioning lines perpendicular to the lines connecting center points. This procedure determines

14 widths and 15 areas in the final image (Figure 3(c) and (d)).

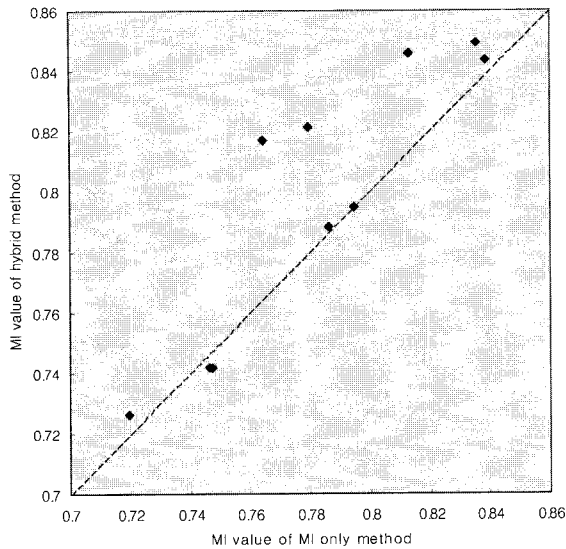


Fig. 7. The similarity of MI method and hybrid method

RESULTS

10 Schizophrenia disease images were compared with 10 normal MRI brain images. For the normalization, each case was registered into brain template introduced in the method section 2-1.

1. Feature similarity constraint parameter

This section shows some effects of the feature constraint parameter λ introduced in the section 2-3. In Figure 4, (h) the image is well registered into the target image for the corpus callosum (dark gray region) and global shape.

2. Comparison of each method of mutual information, Talairach mapping, and our method

Figure 5 shows differences among Talairach mapping, MI, and hybrid methods. The gray indicates the difference between two images, and the white shows the overlapped region of two images. (g) and (h) are well registered into target images about the lateral ventricle and global shape.

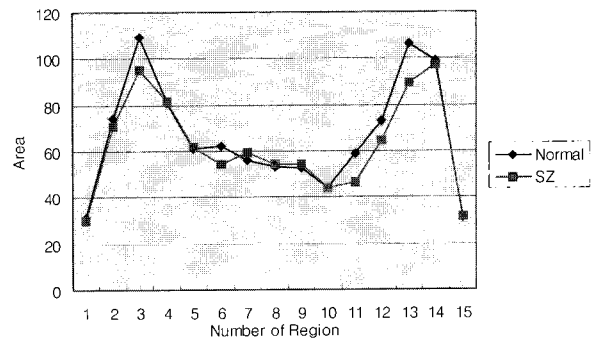


Fig. 8. Average areas of corpus callosum region by section

The result of volume difference estimation between each registered image and target image shows that hybrid registered images ($149280 \pm 9764 \text{mm}^3$) and Talairach space mapped images ($145720 \pm 10700 \text{mm}^3$) have much smaller (about 7.7%) differences than images only using MI maximization ($161780 \pm 11260 \text{mm}^3$). In the one-way ANOVA test, the mean of groups from the hybrid method and the MI only method are significantly different ($p=0.01$).

Figure 6 demonstrates the normalization of the corpus callosum by each method. The white is the overlapped area between floating and reference images, and the gray indicates the difference. (g) and (h) are slightly mismatched in rotation and scaling.

The iteration number of the total cost function is increased in the hybrid method due to refining similarity. But the similarity of mutual information grows up in the hybrid method compared with only the mutual information method as shown in Figure 7. This represents that the hybrid method provides more accurate matching compared with the mutual information method.

3. Schizophrenia detection

Figure 6 shows the comparison of each corpus callosum area measured by Talairach mapping, MI, and hybrid registration. From the t-test, sections of No. 11 and No. 13 are significantly decreased in schizophrenia ($p < 0.01$).

Table 1 shows the difference of global gray matter

Table 1. Difference of global gray matter volume between normal and schizophrenia patient about each method

Method	normal control			schizophrenia		
	Total Area	Gray Matter	GM(%)	Total Area	Gray Matter	GM(%)
Talairach	2301.8 ± 752.6	1312.7 ± 108.5	57.01	2328.2 ± 131.2	1304.3 ± 98.20	56.02
Only MI	1450.1 ± 735.9	852.1 ± 41.84	58.78	1427.4 ± 53.28	813.0 ± 56.24	56.95
Hybrid method	1448.8 ± 536.7	853.7 ± 35.90	58.93	1421.3 ± 82.54	796.3 ± 59.58	56.03

volume between normal and schizophrenia patient. The gray matter volume of schizophrenia patients was shrunk by 0.99%, 1.83%, and 2.90% in Talairach mapping, mutual information, and hybrid registration methods, respectively.

DISCUSSION

The proposed hybrid registration method using mutual information and feature similarity provides a reasonable normalization method for analyzing disease features. In contrast to methods using one of intensity similarity or feature similarity, the algorithm is concerned about local normalization as well as global normalization. The comparison results of each method shows that the normalization of local features such as the corpus callosum is normalized better than mutual information and Talairach mapping methods. It is important to normalize with local feature because local matching affects on the analysis of disease characteristics. Global matching is also important because the GM or CSF area all over brain is a criterion for pathology detection. Our hybrid affine registration method results in allowable global matching.

Comparing it with the mutual information method, the hybrid method increases the intensity similarity value and the iteration number. This result is statistically significant ($p < 0.0001$). The increase of the intensity similarity shows that the global brain is matched better than the mutual information method. However, the refining process with features appears to be too time consuming to converge and to calculate total similarity.

The feature similarity constraint parameter might influence a registration result. The result demonstrates the effect. To match both the feature and intensity distribution, we made the constraint parameter variable. In the experiment, the parameter generally varies from 0.01 of the start to 0.0005 of the final converging.

The corpus callosum, the main fiber tract connecting the two brain hemispheres, which consists of approximately 200–350 million fibers in human, provides the majority of axonal transmissions between the two cerebral hemispheres and subserves interhemispheric information transfer[16]. In this study, we found that the genu of the corpus callosum was smaller in disease patients with Schizophrenia than in normal controls. In contrast, the splenium of the corpus callosum was larger in Schizophrenia disease patients than controls. Decreases in area could be related to underlying decreases in fiber number, in fiber diameter, in non-axonal components resulting in increased fiber

density, mechanical pressure on the corpus callosum from expanding ventricular size, or a combination of these variations.

In the all results by Talairach, mutual information and hybrid methods, the volume of GM is decreased in schizophrenia patients. Global gray matter reduction would be consistent with a widespread disorder of cortical lamination during neurodevelopment. To date, evidence has been found for reductions in global and regional gray matter, and in a number of regions of interest, including the hippocampus, amygdala, superior temporal gyrus and frontal lobe regions[17]. Our method might be adapted to measuring the regional gray matter change by defining appropriate feature points, line, or surface.

In this paper, just 2 features of AC and PC points are used as feature similarity. Many features over two actually may not seriously affect the linear normalization as though defined for feature similarity. However, many feature points are important in the non-linear normalization. If both intensity distribution and feature are used in the nonlinear normalization, the result might provide accurate and reasonable registration for the pathology detection.

CONCLUSIONS

This paper introduced a new affine registration algorithm using both of intensity similarity and feature similarity, and a proposed image analysis method for pathology detection using feature characteristics obtained by comparing the brains to those schizophrenia patients to normal brains. In the future, we will develop a pathology detection method using non-linear deformation registration and deformation field.

Acknowledgement

“This work is the result of research activities of Advanced Biometric Research Center (ABRC) Supported by KOSEF”

REFERENCES

1. P.M. Thompson, M.S. Mega, J. Moussai, S. Zohoori, L.Q. Xu, A. Goldkorn, A.A. Khan, J. Coryell, G. Small, J. Comings, and A.W. Toga, “3D probabilistic atlas and average surface representation of the Alzheimer’s brain, with local variability and proba-

- bility maps of ventricles and deep cortex," in the *Society for Neuroscience*, Washington, DC, USA, 26(2), pp. 1105, Nov. 1996
2. A.W. Toga, P.M. Thompson, B.A. Payne, "Modeling morphometric changes of the brain during development," In: *Developmental Neuroimaging: Mapping the development of brain and behavior*, R.W. Thatcher, G.R. Lyon, J. Rumsey and N. Krasnegor, Academic Press, pp. 15-27, September 1996
 3. R.W. McCarley, C.G. Wible, M. Frumin, Y. Hirayasu, J.J. Levitt, I.A. Fischer, and M.E. Shenton, "MRI anatomy of Schizophrenia," *Biol. Psychiatry*, vol. 45, pp. 1099-1119, 1999
 4. L.G. Brown, "A survey of image registration techniques," *ACM Computing Surveys*, vol. 24, no. 4, pp. 325-376, Dec. 1992
 5. C.R. Maurer and J.M. Fitzpatrick, "A review of medical image registration," in *Interactive Image-Guided Neurosurgery*, R.J. Maciunas, Ed. Park Ridge, IL: Amer. Association of Neurological Surgeons, pp. 17-44, 1993
 6. P.A. van den Elsen, E-J. D. Pol, and M.A. Viergever, "Medical image matching-A review with classification," *IEEE Eng. Med. Biol.*, pp. 26-38, Mar. 1993
 7. J.Y. Chiang and B.J. Sullivan, "Coincident bit counting-A new criterion for image registration," *IEEE Trans. Med. Imag.*, vol. 12, no. 1, pp. 30-38, Mar. 1993
 8. P. Gerlot-Chiron and Y. Bizais, "Registration of multimodality medical images using region overlap criterion," *CVGIP: Graphical Models and Image Processing*, vol. 54, no. 5, pp. 396-406, Sept. 1992
 9. T. Radcliffe, R. Rajapakshe, and S. Shalev, "Pseudocorrelation: A fast, robust, absolute, grey-level image alignment algorithm," *Med. Phys.*, vol. 21, no. 6, pp. 761-769, June 1994
 10. A. Venot, J.F. Lebruchec, and J.C. Roucaurol, "A new class of similarity measures for robust image registration," *Comput. Vision, Graphics, Image Processing*, vol. 28, no. 2, pp. 176-184, Nov. 1984
 11. Frederik Maes, Andre Collignon, Dirk Vandermeulen, Guy Marchal, and Paul Suetens, "Multimodality image registration by maximization of mutual information," *IEEE Trans. Medical Imaging*, vol. 16, no. 2, pp. 187-198, April 1997
 12. Talairach J, Tournoux P, Co-planar stereotaxic atlas of the human brain, New York, Thieme Medical Publishers, pp. 1-20, 1988
 13. W.H. Press, B.P. Flannery, S.A. Teukolsky, and W.T. Vetterling, *Numerical Recipes in C*, 2nd ed. Cambridge, U.K.: Cambridge Univ. Press, ch. 10. pp. 412-419, 1992
 14. Ui Cheul Yoon, Jin Woo Hwang, Jae Seok Kim, Jae Jin Kim, In Young Kim, Jun Soo Kwon, and Sun I. Kim, "Successive fuzzy classification and improved parcellation method for brain analysis," *J. Biomed. Eng. Res.*, Vol. 22, No. 4, pp. 238-240, 2001
 15. James C. Bezdek, *Pattern Recognition with Fuzzy Objective Func Algorithms*, Plenum Press, New York, pp. 64-86, 1981
 16. F. Aboitiz, A.B. Scheibel, R.S. Fisher, E. Zaidel, "Fiber composition of the human corpus callosum," *Brain Res.*, Dec. vol.11:598(1-2), pp. 143-153, 1992
 17. I.C. Wright, Z.R. Ellison, T. Sharma, K.J. Friston, R.M. Murray, P.K. McGuire, "Mapping of grey matter changes in schizophrenia," *Schizophrenia Research*, vol. 35, pp. 1-14, 1999